Journal of Crystal Growth 126 (1993) 125–132
North-Holland

JOURNAL OF CRYSTAL GROWTH

Mechanisms of strain relaxation in III–V semiconductor heterostructures

M. Mazzer, F. Romanato, A.V. Drigo and A. Carnera

Unità GNSM – INFM, Dipartimento di Fisica, Università di Padova, Via Marzolo 8, I-35131 Padova, Italy

The known models describing the breakdown of coherency between layer and substrate in mismatched heterostructures are based on the isotropic elastic continuum approximation. As a matter of fact an internal contribution to the misfit accommodation, that is a deviation from the so-called "virtual crystal approximation", is expected in ternary or more complex alloy structures. This effect is clearly seen in a set of $In_xGa_{1-x}As/GaAs$ low misfit samples in the presence of misfit dislocations. The complete structural characterisation including the elastic distortion field and the dislocation density and distribution has been performed by means of Rutherford backscattering based techniques and double crystal X-ray diffraction.

1. Introduction

The structural and thermodynamical properties of III–V semiconductor strained heterostructures are still a developing subject. As far as strained heterostructures are concerned, two main problems have to be considered from the structural point of view. The first is the limit to strained layer reachable achievable thickness given by the generation of misfit dislocations at the interface between film and substrate above the so-called critical thickness. As the dislocations highly affect the electrical efficiency of the semiconductor devices, their generation mechanisms must be clearly understood. The second problem concerns the need for buffer layers which could interface highly mismatched materials by completely relaxing the strain or confine the dislocations in the intermediate layers. In this way the upper layer can be grown unstrained on a defect-free surface without any limitation for the total thickness. Because of this, strain relaxation mechanisms and defect multiplication processes, which can suggest a method of confining the dislocations by means of some propagation barriers, are very important subjects of investigation. At present there are still no theoretical or phenomenological models which can fully explain the behaviour of semiconductor heterostructure from both the point of view of the the thermodynamic stability and the defect kinetics.

In this paper we pay attention to some of the still open topics in connection with the latest developments of Rutherford backscattering spectrometry (RBS) based characterization techniques. Experimental results concerning a set of $In_xGa_{1-x}As/GaAs$ low misfit samples are discussed in detail. Finally, a general phenomenological approach is considered which can overcome some of the drawbacks of the models based on the isotropic elastic continuum approximation.

2. The effect of misfit dislocation

Many of the unanswered questions are related to the effect of misfit dislocations (plastic deformation) in misfit accommodation. It is important to notice that misfit dislocations must play an important role, not only in reducing the elastic strain energy, but also in changing the lattice configuration by gradually relaxing constraints imposed by the substrate.

In low misfit heterostructures ($f < 1$–2%), misfit lines make up a sort of quasi-planar grid lying at the interface between film and substrate. This grid is generally confined within a narrow region as confirmed by TEM images [1]. The

0022-0248/93/$06.00

effects of a planar grid of dislocations have been studied within the linear elasticity theory of an isotropic continuum [2]. The total elastic distortion field including plastic contribution of the dislocations turns out to depend on 6 parameters which are linear combinations of the components of the average Burgers vectors calculated for each array of parallel misfit lines. The average Burgers vector $\boldsymbol{b}$ for a given line orientation is calculated by summing up all the observed Burgers vectors $\boldsymbol{B}_i$ weighted by the respective line density $n(\boldsymbol{B}_i)$, that is

$$\boldsymbol{b} = \sum \boldsymbol{B}_i \, n(\boldsymbol{B}_i).$$

We consider (001) grown heterostructures, but

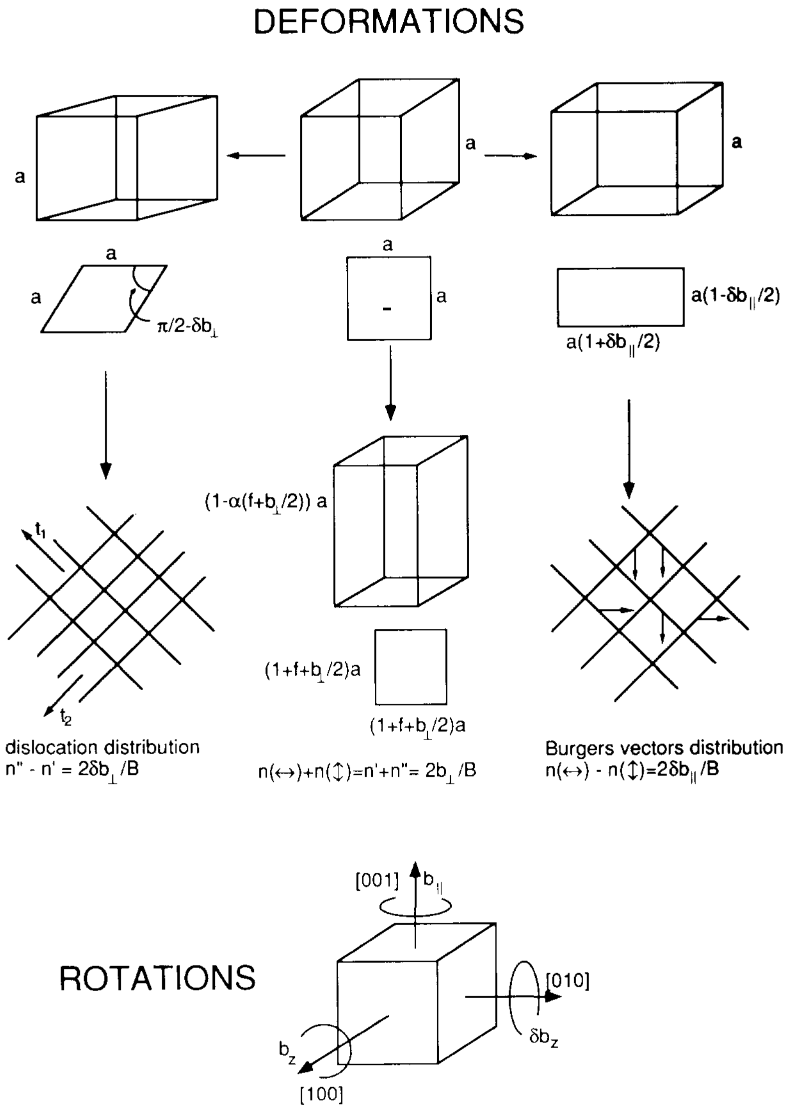

Fig. 1. Cubic lattice distortions for a (001) grown heterostructure in the presence of misfit dislocations: (a) tetragonal distortion (at the centre) depending on the total number of dislocations per unit length at the interface; (b) monoclinic deformation related to the unbalance of the dislocation densities in $\boldsymbol{t}_1 = [110]$ and $\boldsymbol{t}_2[1\bar{1}0]$ direction; (c) orthorhombic deformation related to the unbalance of dislocation densities having Burgers vector in (100) and (010) planes.

the calculations are easily extendable to other growth directions. In this case the dislocations are distributed along the two directions $\boldsymbol{t}_1 = [110]$ and $\boldsymbol{t}_2 = [1\bar{1}0]$ in the growth plane. Both of the average Burgers vectors $\boldsymbol{b}_1$ and $\boldsymbol{b}_2$ can be written as the sum of three independent components, the first being the screw component $\boldsymbol{b}_{i\|} = \boldsymbol{b}_i \cdot t_i$, whilst the second and the third are the projection of the edge component on the growth plane ($\boldsymbol{b}_{i\perp}$) and on the perpendicular direction ($\boldsymbol{b}_{iz}$), respectively. In this case the 6 parameters quoted above are:

$$b_\| = b_{1\|} + b_{2\|}, \qquad \delta b_\| = b_{2\|} - b_{1\|},$$
$$b_\perp = b_{1\perp} + b_{2\perp}, \qquad \delta b_\perp = b_{2\perp} - b_{1\perp},$$
$$b_z = b_{1z} + b_{2z}, \qquad \delta b_z = b_{2z} - b_{1z}. \tag{1}$$

Apart from some lateral non-uniformity, which vanishes at a distance from the dislocation plane that is comparable to the grid spacing [2], the total elastic distortion tensor u is the sum of three terms:

$$\mathrm{u} = \boldsymbol{\varepsilon}^{\mathrm{e}} + \boldsymbol{\varepsilon}^{\mathrm{p}} + \mathrm{R}^{\mathrm{p}}, \tag{2}$$

where

$$\boldsymbol{\varepsilon}^{\mathrm{e}} = \begin{pmatrix} f & 0 & 0 \\ 0 & f & 0 \\ 0 & 0 & -\alpha f \end{pmatrix} \tag{3}$$

is the purely elastic term containing the misfit f between film and substrate. The two other tensors give the plastic contribution:

$$\boldsymbol{\varepsilon}^{\mathrm{p}} = \frac{1}{2}\begin{pmatrix} b_\perp & 0 & 0 \\ 0 & b_\perp & 0 \\ 0 & 0 & -\alpha b_\perp \end{pmatrix} + \frac{1}{2}\begin{pmatrix} \delta b_\| & 0 & 0 \\ 0 & -\delta b_\| & 0 \\ 0 & 0 & 0 \end{pmatrix} + \frac{1}{2}\begin{pmatrix} 0 & \delta b_\perp & 0 \\ \delta b_\perp & 0 & 0 \\ 0 & 0 & 0 \end{pmatrix}, \tag{4}$$

$$\mathrm{R}^{\mathrm{p}} = \frac{1}{2}\begin{pmatrix} 0 & b_\| & 0 \\ -b_\| & 0 & 0 \\ -0 & 0 & 0 \end{pmatrix} + \frac{1}{2}\begin{pmatrix} 0 & 0 & \sqrt{2}\,\delta b_z \\ & 0 & 0 \\ -\sqrt{2}\,\delta b_z & 0 & 0 \end{pmatrix} + \frac{1}{2}\begin{pmatrix} 0 & 0 & 0 \\ 0 & 0 & \sqrt{2}\,b_z \\ 0 & -\sqrt{2}\,b_z & 0 \end{pmatrix}. \tag{5}$$

The symmetric tensor $\boldsymbol{\varepsilon}^{\mathrm{p}}$ is the plastic strain which describes three independent deformations of the lattice primitive cell (fig. 1). The first term on the right side of eq. (4) looks like the elastic term and gives the tetragonal distortion reduction due to the dislocations. The second and the third terms involve the base of the unit cell describing the transition from cubic to orthorhombic and from cubic to monoclinic structures. Finally, each term of the antisymmetric tensor R^{p} describes the rotation of the film cells about one of the $\langle 100 \rangle$ directions with respect to the substrate.

It is well known that in ((001) grown) low misfit systems, misfit dislocations are mainly of 60° type. This means that for each dislocation orientation, Burgers vectors are along the four $\langle 110 \rangle$ directions inclined to the interface. Half of the possible Burgers vectors are contained in (100) plane ($\boldsymbol{B}_{(100)}$ group) and the others in (010) plane ($\boldsymbol{B}_{(010)}$ group). Taking into account these properties, a straightforward calculation [2] provides the link between the three degrees of freedom of the strain field (eq. (4)) and the dislocation distributions with respect to the orientation of both the misfit lines and Burgers vectors. Let n_1 and n_2 be the number of dislocation per unit length in $\boldsymbol{t}_1$ and $\boldsymbol{t}_2$ direction, respectively, and let $n(\boldsymbol{B}_{(100)})$ and $n(\boldsymbol{B}_{(010)})$ be the number of dislocations per unit length whose Burgers vectors lay in (100) and in (010) plane no matter what the line orientation is. It turns out that [4]:

$$\delta n = n_2 - n_1 = \frac{2\sqrt{2}}{a}\delta b_\perp, \tag{6}$$

$$\delta^* n = n(\boldsymbol{B}_{(100)}) - n(\boldsymbol{B}_{(010)}) = \frac{2\sqrt{2}}{a}\delta b_\|, \tag{7}$$

$$n_{\mathrm{tot}} = n_2 + n_1 = n(\boldsymbol{B}_{(100)}) + n(\boldsymbol{B}_{(010)}) = \frac{2\sqrt{2}}{a} b_{\perp} . \tag{8}$$

These formulae show the complete link between lattice deformations and dislocation distributions (fig. 1). These results are valid for an isotropic elastic continuum and their reliability depend on the investigated structure. For monoelemental layers or for binary compounds no appreciable deviation from eqs. (2)–(7) is expected but alloys can exhibit a quite different behaviour, as discussed in sections 4 and 5.

3. Characterization techniques

For the complete structural characterization of a single layer heterostructure, the misfit between layer and substrate, the complete elastic distortion field and the dislocation distribution and density must be measured independently.

RBS is a good technique to measure the alloy composition in a wide range of conditions. We have worked out a program for the simulation of a RBS spectrum which uses the composition x as a fitting parameter. By the comparison between the experimental and the simulated spectra, we can determine x with good precision. For instance, in a InGaAs/GaAs system the precision is better than 0.5 at%; assuming Vegard's law, the knowledge of the composition is sufficient to calculate the heterolayer misfit.

RBS channelling, in turn, allows us to detect the complete set of lattice deformations (tetragonal distortion plus the deformations of the cell base) by measuring a sufficient number of angles between couples of different axial or planar channelling directions. This is done with a precision of about 0.02° by using a goniometer which has been designed in order to allow independent rotations around three axes with a precision and repeatability of 0.01° [3]. The strain sensitivity turns out to about 3×10^{-4}, which is a good value for the analysis of the strain release in samples having a misfit of the order of 10^{-2}. This sensitivity is comparable to the best double crystal X-ray diffractometry (DCD) precisions for single layer heterostructures and, contrary to DCD, it is independent of the layer thickness. The main advantage of X-ray diffractometry is the possibility to detect at the same time not only the three deformation parameters, but also the three rotations [4]. As a matter of fact, it is possible to discriminate the epilayer deformations in the growth plane and in the perpendicular direction, since the signal coming from the layer can be compared to the one coming from the substrate at the same time. This is not so for RBS channelling, which cannot investigate the strain field in buried layers because of the so-called steering effect [5]. This is the reason that makes DCD suitable for detecting any failure of the isotropic elastic continuum model. This topic is considered in detail in section 5.

From the defect characterization point of view, the dechannelling technique allows us to obtain direct information on the misfit dislocations [1]. This information is independent of the strain characterization data, since the latter provide a picture of the average elastic field far from the dislocation cores, whilst the dechannelling events are related to the strong elastic fields close to each dislocation line. The analysis of RBS spectra under channelling conditions allows one to obtain the dislocation densities by a comparison with a perfect crystal spectrum used as a reference. Since the same dislocation gives different contributions to the backscattering yield, depending upon the channelling conditions, it is possible to characterize the dislocation network by simply playing with the channelling geometry [6]. The overall sensitivity in the dislocation density measurements turns out to be better than 10^{-4} lines cm^{-1}, which is a good result with respect to any indirect estimation obtained, for instance, from strain data. The limit of this technique is at high dislocation densities where the dechannelling contributions of two adjacent dislocations can no longer be resolved.

4. Experimental results

A set of $In_xGa_{1-x}As/GaAs$ samples having different composition ($0.035 \le x \le 0.15$), i.e., different misfit ($2.5 \times 10^{-3} \le f \le 1.07 \times 10^{-2}$), have been analysed by RBS channelling and DCD [5]. Three main experimental results can be pointed out. The first concerns the existence of two different critical thicknesses. The first critical thickness, T_c, is related to the onset of misfit dislocation generation and turns out to be in agreement with the prediction of the equilibrium theories of Matthews and Blakeslee [8] and Van der Merwe [9]. Despite the fact that misfit dislocations actually appear above T_c, no appreciable strain reduction is observed below a second critical thickness, T_c' (fig. 2). The difference between T_c and T_c' values is remarkable and it can reach one order of magnitude. From T_c to just above T_c', dislocations are mainly observed in one direction, as confirmed by RBS dechannelling [7].

As a second outcome, it can be asserted that above T_c' the residual strain for a particular system is clearly a unique function of the epilayer thickness, as shown in fig. 2. The rate of strain reduction with increasing layer thickness is well below the prediction of the equilibrium theories. This conclusion is supported by a greater amount of experimental data concerning samples having different composition and grown in quite dissimilar conditions [5]. The results of our annealing experiments [5] are also in contradiction with the hypothesis of metastability suggested by some authors.

The third item is still a matter of discussion. As a matter of fact, the tetragonal ratio $\eta = a_\perp/a_\parallel$ measured by RBS channelling always agrees with the ratio between the two independent quantities $a_\perp$(DCD) and $a_\parallel$(DCD) obtained by DCD within the experimental errors. In an isotropic elastic material, the in-plane strain $\varepsilon_\parallel^{\text{iso}}$ is given by:

$$\varepsilon_\parallel^{\text{iso}} = \frac{1-\eta}{\alpha+\eta}, \tag{9}$$

where α is obtainable from the cubic elastic constants and depends on the growth direction [10] (in particular for (001) grown layers we have $\alpha = 2C_{12}/C_{11}$). Therefore, if the isotropy approximation is assumed, we have $\varepsilon_\parallel^{\text{iso}}(\text{RBS}) \approx \varepsilon_\parallel^{\text{iso}}(\text{DCD})$.

However, if the in-plane strain $\varepsilon_\parallel(\text{DCD}) = [a_\parallel(\text{DCD}) - a(x)]/a(x)$ and the perpendicular

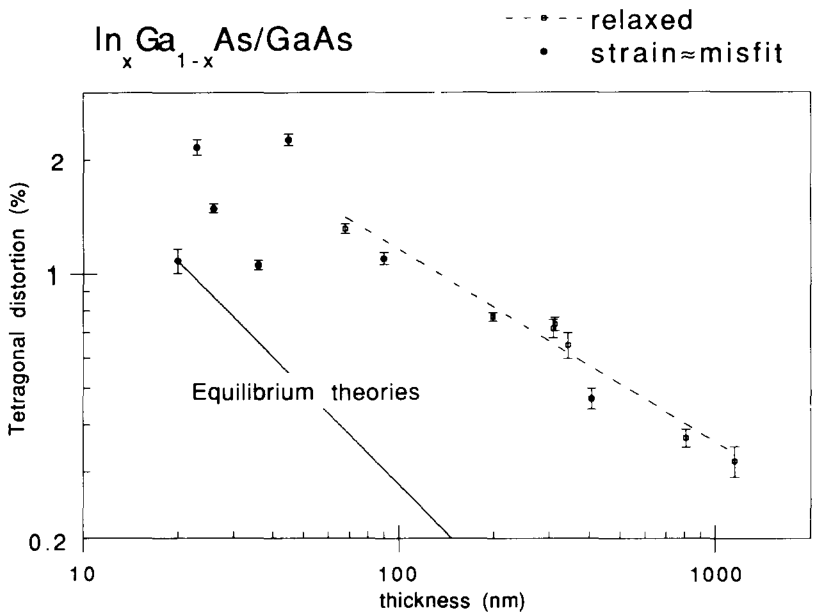

Fig. 2. Tetragonal distortion $(1-\eta)$, where $\eta = a_\perp/a_\parallel$ is the tetragonal ratio measured by RBS channelling, as a function of the sample thickness. The circles indicate the unrelaxed samples, whilst the squares show the samples where a detectable distortion release has been measured.

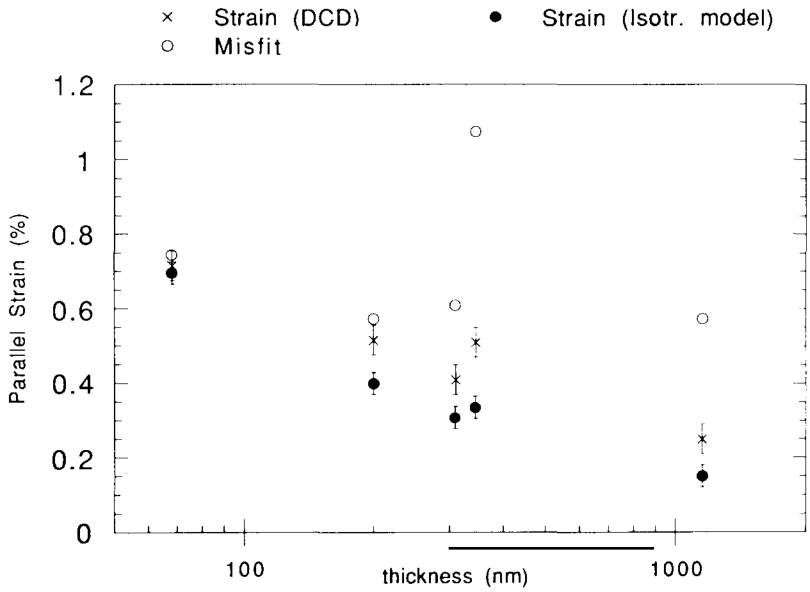

Fig. 3. Parallel strain as measured by DCD compared to the values obtained from the tetragonal ratio as measured by RBS channelling. In the second case, isotropy approximation has been assumed.

strain $\varepsilon_{\perp}(\mathrm{DCD}) = [a_{\perp}(\mathrm{DCD}) - a(x)]/a(x)$ are calculated from the respective lattice parameters obtained by DCD, it turns out that, at least for the analysed InGaAs/GaAs samples in the presence of misfit dislocations, the predictions of the isotropic elastic continuum model are in general not satisfied, that is:

$$\varepsilon_{\perp}(DCD)/\varepsilon_{\parallel}(DCD) \neq \alpha. \tag{10}$$

These results are shown in fig. 3 where the strain calculated by using eq. (9) (based on the isotropy

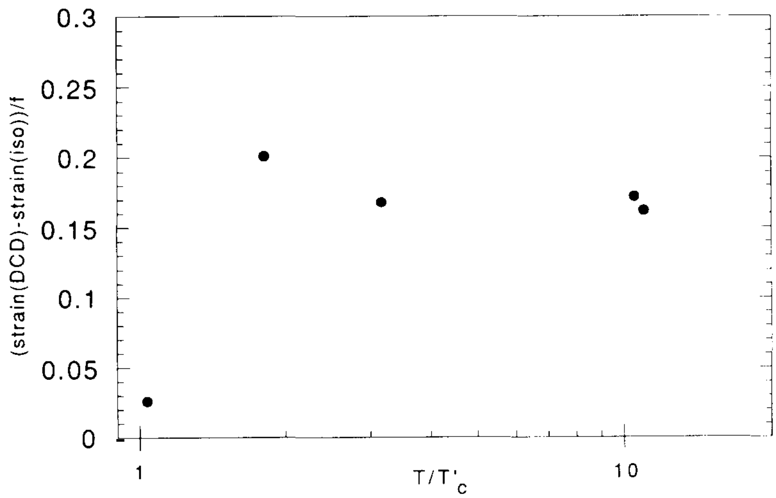

Fig. 4. Relative strain difference as a function of the ratio between the sample thickness and the critical thickness T_c'.

approximation) is compared to $\varepsilon_{\parallel}$(DCD) for different sample thickness. It is evident that the difference is well beyond the experimental uncertainties for all the sample except one. The analysed samples do not have the same misfit (see fig. 3), so the trend can be brought to light by plotting the quantity $[\varepsilon_{\parallel}^{\text{iso}} - \varepsilon_{\parallel}(\text{DCD})]/f$ (f is the misfit) as a function of the ratio T/T_c' between the sample thickness and the critical thickness (fig. 4). The relative difference between the two determinations of $\varepsilon_{\parallel}$ turns out to be negligible below T_c', whilst it seems to be stronger just above T_c' and then to saturate at a value of about 15–20%.

5. Discussion

Failures of the isotropic elastic continuum model are evident in III–V semiconductor heterostructures when the critical thickness for strain relaxation T_c' is approached. As pointed out before, the asymmetry in the misfit line distribution, which is appreciable not only between T_c and T_c', but also for thickness values up to $T \approx 2T_c'$, introduces a new kind of deformation involving a changing in shape of the primitive cell basis, i.e., the cell deformation ceases to be purely tetragonal. In this case, three independent physical parameters are necessary for a complete description of the elastic distortion field induced by the dislocations. In other words, the film lattice is no longer forced to maintain the simple tetragonal form imposed by the substrate and it has three degrees of freedom at its disposal to accommodate the mismatch.

In an isotropic elastic continuum, the three deformations are completely independent (see eq. (4)). For instance, the tetragonal distortion cannot be compensated by a deformation of the cell base from the elastic energy point of view. However, the so-called virtual crystal approximation, namely the application of Vegard's law to bond lengths in alloys, turns out to be an oversimplification. In fact EXAFS experiments [11] show that bond lengths in the alloys do not follow Vegard's law, which in turn is a rather good rule for the average lattice parameter. Bond lengths and angles vary to a much lower extent, remaining closer to the corresponding binary compound values [12]. It follows that the actual crystal structure is related to the bond tetrahedra accommodation with the minimum distortion. The Keating model [13] provides an algorithm for the calculation of the elastic energy, which is based on the knowledge of the bond force constants. By using this model, Mbaye et al. [14] have shown that for certain composition values, ternary alloys may crystallize in highly ordered structures where sublattices containing atoms of different species can be resolved into homogeneous sublattices of lower order. For instance, this is the case of chalcopyrite or CuAu-like lattices when alloys of the type $A_{0.5}B_{0.5}C$ are involved. In ordered structures of this kind the substrate misfit can be accommodated not only by tetragonal distortion, but also by internal displacements of the distinct monoelemental sublattices.

The isotropic elastic continuum cannot account for this internal degree of freedom, which may be very effective in reducing the elastic energy of the epitaxial film. In particular, it can be shown that the minimum energy of the structure does not correspond to the absence of tetragonal distortion and the relation between in-plane and perpendicular strains may differ remarkably from the isotropic continuum model prediction. If the alloy is not ordered, this effect is expected to be weaker. However, the above mechanism still works and the layer structure may be thought if as a statistically weighted superposition of ordered clusters. It has been shown that this approach provides a good picture of the actual distribution of bond lengths [15] and can be the starting point for the understading of misfit accommodation mechanisms by means of both elastic and plastic deformations.

Mbaye et al. [14] suggest the existence of what they calls "selection of species" induced by the misfit. That is, the actual arrangement of bond tetrahedra should depend strongly on the substrate constraint and the overall effect on the elastic energy density can be strong enough to invalidate the energy minimization calculations performed within the VCA model, for instance the equilibrium theories of Matthews and Blakeslee.

A satisfactory model for misfit accommodation in epitaxial systems involving ternary alloys has not been proposed yet. However, some conclusions may be drawn on the basis of what has just been discussed. Coming back to the dislocation contribution to strain relaxation, the DCD data on parallel and perpendicular lattice parameters, whose behaviour is not fitted by the isotropic continuum model, can be read as follows. Before the onset of misfit dislocation generation, i.e., under coherency conditions, the discrepancies between the experimental data and the isotropic model are negligible within experimental uncertainties, suggesting that the internal degrees of freedom of the layer structure are somehow frozen, perhaps because of the substrate constraint. Above the critical thickness T_c, the dislocations begin to break the coherency and the three "external" degrees of freedom (relative to the average structure of the fundamental cell) interfere with the "internal" ones, causing a relaxation of tetragonal distortion which is not justified by the in-plane strain reduction alone. In particular, the dislocation density unbalance with respect to the line orientations in the growth plane, which is responsible for monoclinic deformation of the unit cell, seems to give the main indirect contribution to the enhancement of the internal misfit accommodation efficiency.

6. Conclusions

Structural characterization of low misfit epitaxial heterostructures gives evidence that important mechanisms of misfit accommodation are not consistent with models based on the isotropic elastic continuum approximation. Discrepancies are expected to be stronger for ternary alloy epilayers or more complex structures. A set of low misfit InGaAs/GaAs single layer structures has been characterized by RBS channelling and DCD. The experimental results suggest that the breakdown of the isotropy approximation is due mainly to the generation of misfit dislocations which relax the constraints imposed by the substrate. Work is in progress in order to develop a phenomenological model describing the combined effects of the plastic deformation and the internal mechanisms of misfit accommodation.

Acknowledgements

We thank Dr. P. Franzosi, Dr. C. Ferrari, Dr. G. Salviati and Dr. L. Lazzarini from MASPEC–CNR for DCD measurements and for TEM images. This work has been supported by the Finalized Project Materials and Devices for Solid State Electronics of Consiglio Nazionale delle Ricerche (CNR).

References

[1] G. Salviati, C. Ferrari, A.V. Drigo, F. Romanato and F. Genova, in: Proc. 17th Congr. on Electron Microscopy, Italian Society, Lecce, 1989, p. 273.
[2] M. Mazzer, A. Carnera, A.V. Drigo and C. Ferrari, J. Appl. Phys. 68 (1990) 531.
[3] A. Carnera and A.V. Drigo, Nucl. Instr. Methods B 44 (1990) 357.
[4] M. Mazzer, in: Condensed Systems of Low Dimensionality, Ed. J.L. Beeby (Plenum, New York, 1991) p. 461.
[5] A.V. Drigo, A. Aydinly, A. Carnera, F. Genova, C. Rigo, C. Ferrari, P. Franzosi and G. Salviati, J. Appl. Phys. 66 (1989) 1975.
[6] F. Romanato, M. Mazzer and A.V. Drigo, Nucl. Instr. Methods B 63 (1992) 36.
[7] M. Mazzer, A.V. Drigo and F. Romanato, Nucl. Instr. Methods B 64 (1992) 103.
[8] J.W. Matthews, S. Mader and T.B. Light, J. Appl. Phys. 41 (1970) 3800.
[9] J.H. van der Merwe and C.A. Ball, in: Epitaxial Growth, Part B, Ed. J.W. Matthews (Academic Press, New York, 1975) ch. 6.
[10] J. Hornstra and W.J. Bartels, J. Crystal Growth 44 (1978) 513.
[11] J.C. Mikkelsen, Jr. and J.B. Boyce, Phys. Rev. B 28 (1983) 7130.
[12] J.L. Martins and A. Zunger, Phys. Rev. B 30 (1984) 6217.
[13] P.N. Keating, Phys. Rev. B 30 (1984) 6217.
[14] A.A. Mbaye, D.M. Wood and A. Zunger, Phys. Rev. B 37 (1988) 3008.
[15] A. Zunger and D.M. Wood, J. Crystal Growth 98 (1989) 1.